

# Appendix B for

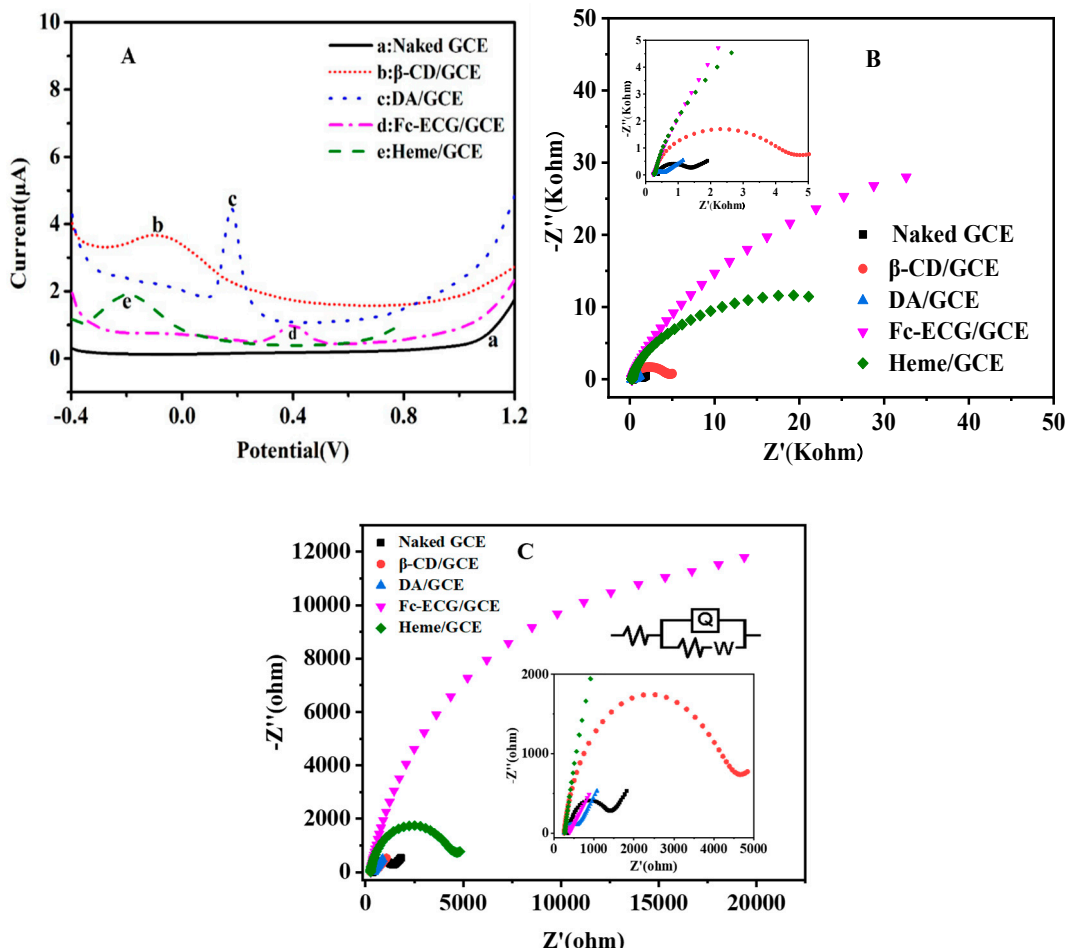
## Convenient Heme Nanorod Modified Electrode for Quercetin Sensing by Two Common Electrochemical Methods

Jin-Guang Liu <sup>†</sup>, Jia-Zheng Wan <sup>†</sup>, Qing-Min Lin, Guo-Cheng Han\*, Xiao-Zhen Feng\* and Zhencheng Chen\*

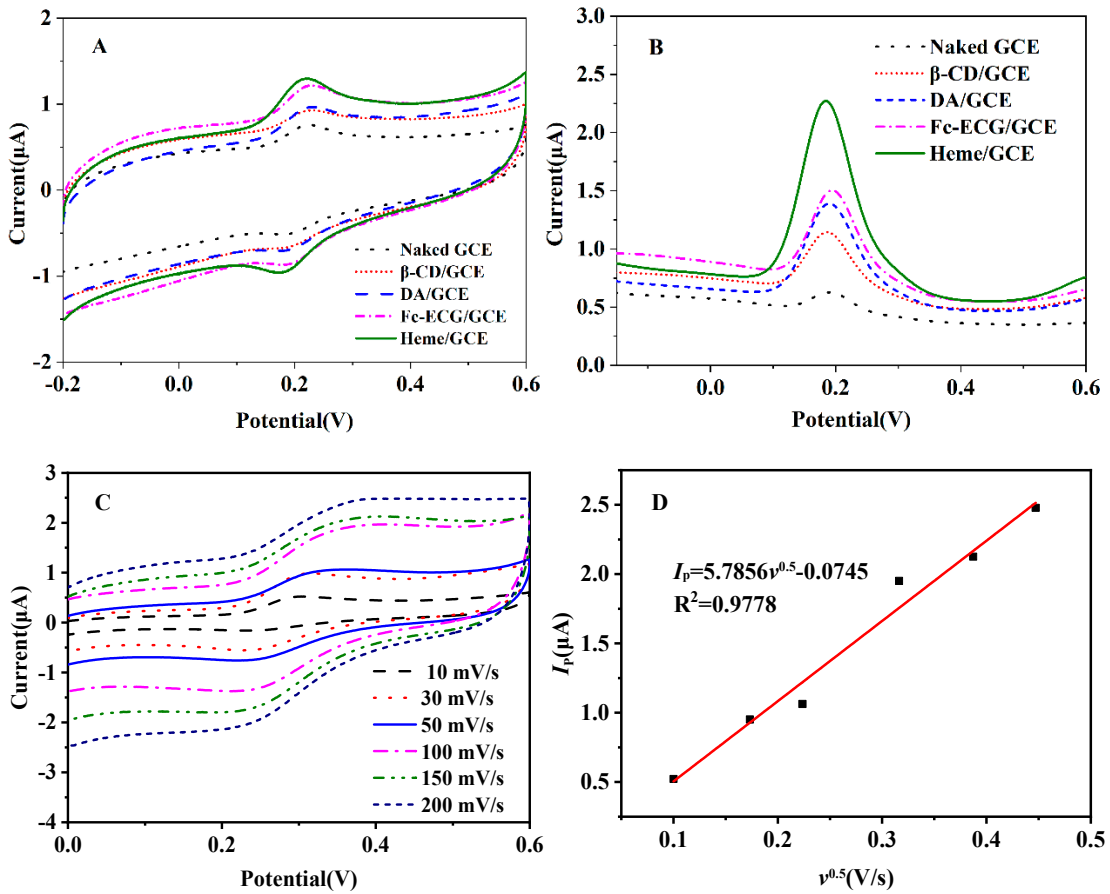
School of Life and Environmental Sciences, Guilin University of Electronic Technology, Guilin 541004, P. R. China; [liujg124879892@163.com](mailto:liujg124879892@163.com) (J.-G. L.); [a1197797116@163.com](mailto:a1197797116@163.com) (J.-Z. W.); [lqm442049752@163.com](mailto:lqm442049752@163.com) (Q.-M. L.)

\* Correspondence: [hangc81@guet.edu.cn](mailto:hangc81@guet.edu.cn) (G.-C. H.), [fxz97118@guet.edu.cn](mailto:fxz97118@guet.edu.cn) (X.-Z. F.) and E-mail: [chenzhch1965@163.com](mailto:chenzhch1965@163.com) (C. Z. C.).

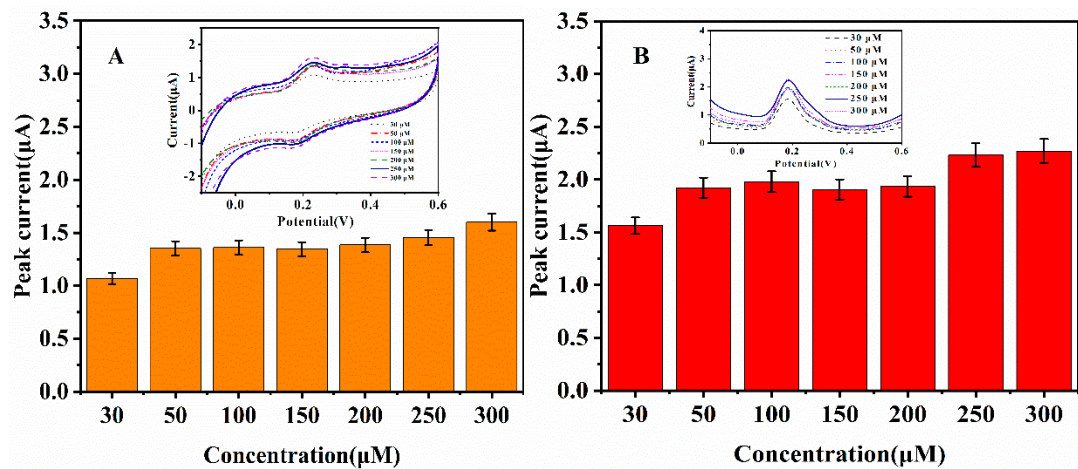
<sup>†</sup> These authors contributed equally to this work.

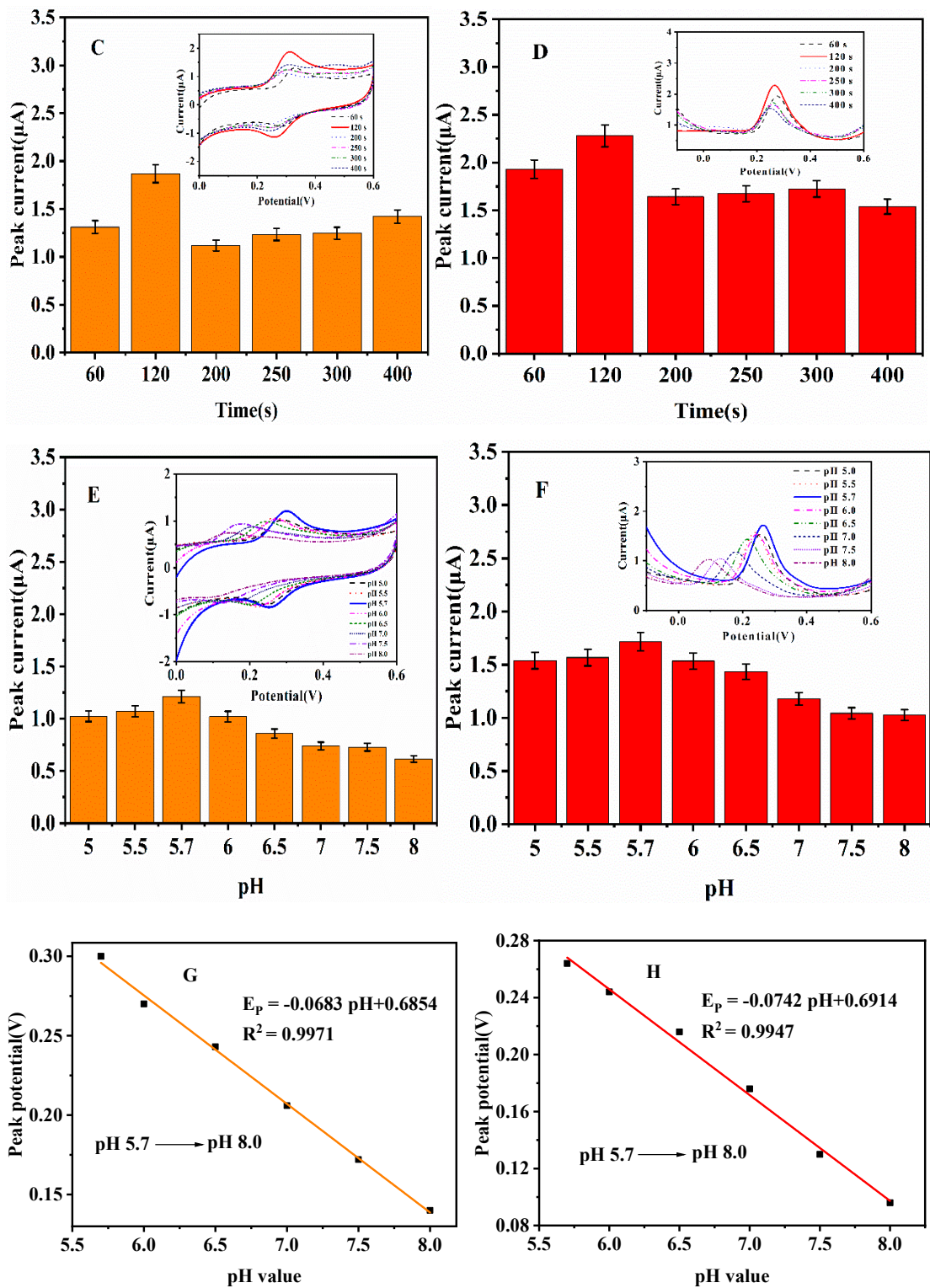


**Figure S1:** DPV graphs (A) of different working electrodes in PBS buffer (pH 7.0) and EIS diagrams (B) of different working electrodes in  $5 \text{ mmol}\cdot\text{L}^{-1} \text{K}_3[\text{Fe}(\text{CN})_6]/\text{K}_4[\text{Fe}(\text{CN})_6]$  solution; EIS fitting diagrams (C).



**Figure S2:** CV (A) and DPV (B) diagrams of  $10 \mu\text{mol}\cdot\text{L}^{-1}$  Qu on different working electrodes; (C) Cyclic voltammograms of Qu at Heme/GCE with different scan rate (10–200 mV/s); (D) The plots of anodic peak currents ( $I_p$ ) and Qu vs.  $v^{0.5}$ .





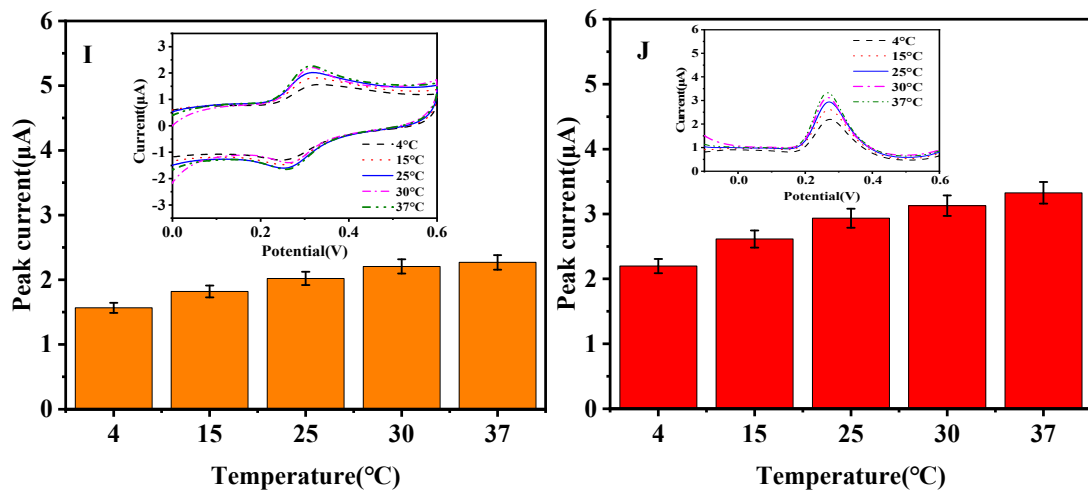


**Figure S3:**  $10 \mu\text{mol}\cdot\text{L}^{-1}$  Qu on working electrodes modified with different Heme concentrations (A) CV graph and (B) DPV graph; (C) CV graph and (D) DPV graph of the  $10 \mu\text{mol}\cdot\text{L}^{-1}$  Qu under different Heme deposition time; (E) CV graph and (F) DPV graph of the  $10 \mu\text{mol}\cdot\text{L}^{-1}$  Qu detected in PBS buffer with different pH; (G) The relationship between peak potential and pH value in CV method; (H) The relationship between peak potential and pH value in DPV method; (I) CV graph and (J) DPV graph of the  $10 \mu\text{mol}\cdot\text{L}^{-1}$  Qu at different temperatures.

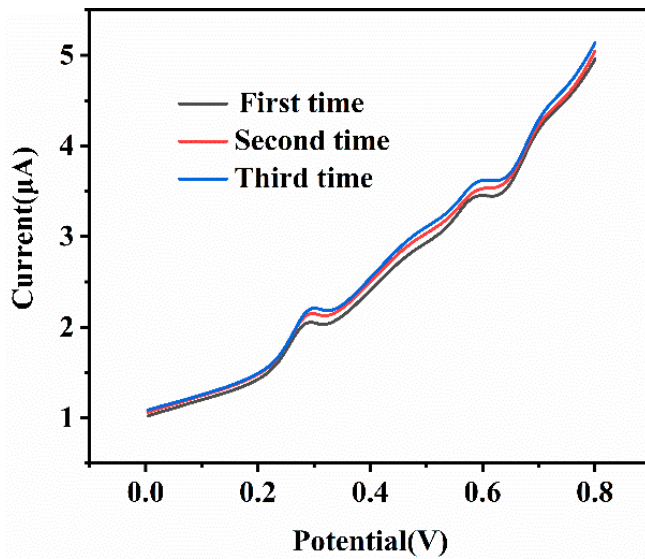


**Figure S4:** The DPV diagram of the actual sample tested three times in a row.

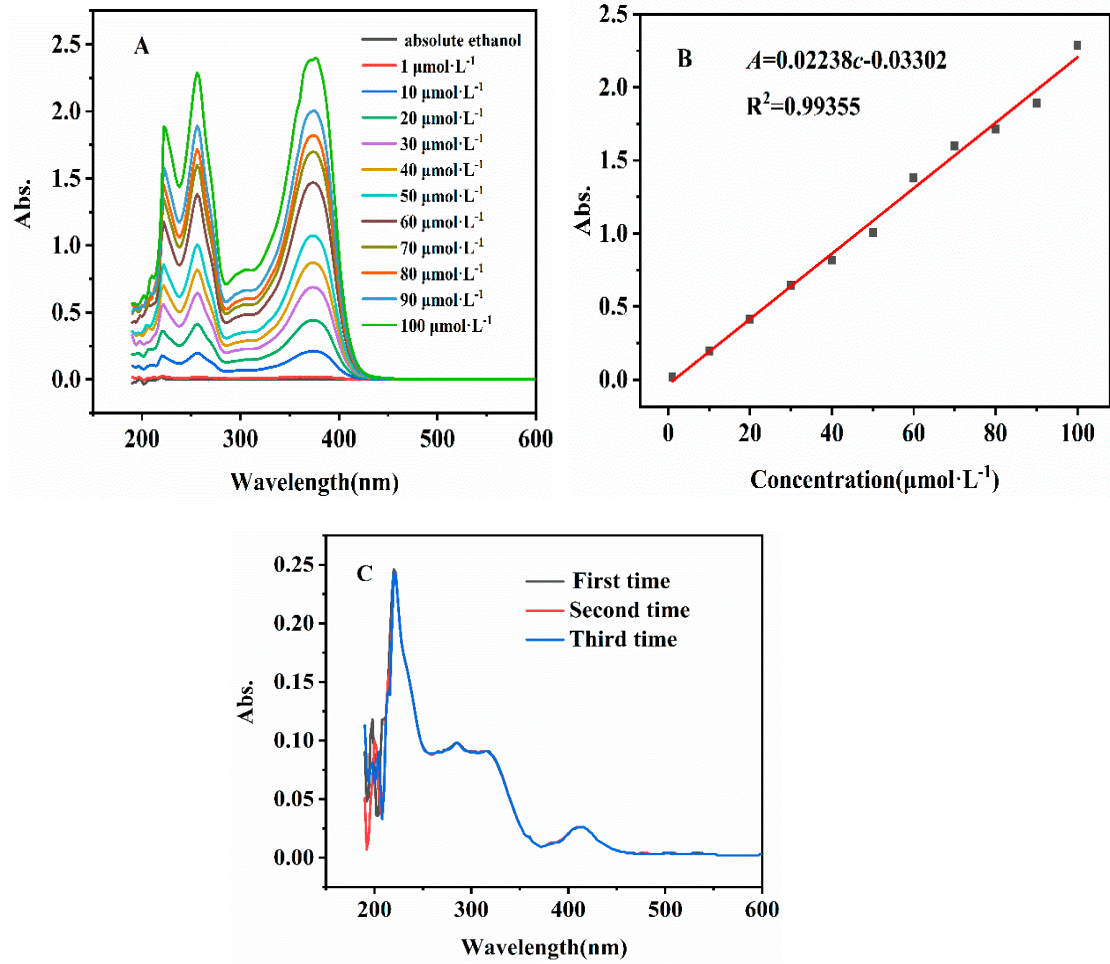


**Figure S5:** (A) UV-Vis spectra of different concentration of standard Qu solution, (B) the linear fitting curve of UV detection, and (C) UV-Vis spectra of actual samples were detected by three times.

**Table S1: Comparison with other Qu detection methods**

Electrode	Detection method	Scope of test ( $\mu\text{M}$ )	Detection limit ( $\mu\text{M}$ )	References
ZnO/CNS/MCPE/GCE	DPV	0.17-3.63	0.04	[1]
MIP/GO/GCE	CV	0.1-100	0.065	[2]
EDS/MCNTs/GCE	CV	0.995-47.6	0.036	[3]
Fe <sub>3</sub> O <sub>4</sub> @ZnO/CP/GCE	CV	0.79-61	0.16	[4]
Mn-doped/ZnS/QDs/GCE	DPV	0.33-20	0.16	[5]
MnWO <sub>4</sub> /GCE	CV	16.7-74.4	-	[6]
WS <sub>2</sub> /GCE	DPV	5.0-1000	1.20	[7]
MIP/MIL-101(Cr)/MoS <sub>2</sub> /GCE	DPV	0.1-700	0.02	[8]

Heme/GCE	DPV	0.1-700	0.063	this work
	CV	0.1-700	0.134	

## References

- Saritha, D.; Koirala, A. R.; Venu, M.; Reddy, G. D.; Reddy, A. V. B.; Sitaram, B.; Madhavi, G.; Aruna, K., A simple, highly sensitive and stable electrochemical sensor for the detection of quercetin in solution, onion and honey buckwheat using zinc oxide supported on carbon nanosheet (ZnO/CNS/MCPE) modified carbon paste electrode. *Electrochim. Acta* **2019**, *313*, 523-531. <https://doi.org/10.1016/j.electacta.2019.04.188>.
- Sun, S.; Zhang, M.; Li, Y.; He, X., A molecularly imprinted polymer with incorporated graphene oxide for electrochemical determination of quercetin. *Sensors* **2013**, *13*, 5493-506. <https://doi.org/10.3390/s130505493>.
- Zheng, Y.; Ye, L.; Yan, L.; Gao, Y., The Electrochemical Behavior and Determination of Quercetin in Choline Chloride/Urea Deep Eutectic Solvent Electrolyte Based on Abrasively Immobilized Multi-Wall Carbon Nanotubes Modified Electrode. *Int. J. Electrochem. Sci.* **2014**, *9*, 238-248. <https://doi.org/10.1149/2.006402eeel>.
- Arvand, M.; Chaibakhsh, N.; Daneshvar, S., Amperometric Determination of Quercetin in Some Foods by Magnetic Core/Shell Fe<sub>3</sub>O<sub>4</sub>@ZnO Nanoparticles Modified Glassy Carbon Electrode. *Food Anal. Methods* **2015**, *8*, 1911-1922. <https://doi.org/10.1007/s12161-014-0080-8>.
- Zhang, Z.; Miao, Y.; Lian, L.; Yan, G., Detection of quercetin based on Al<sup>3+</sup>-amplified phosphorescence signals of manganese-doped ZnS quantum dots. *Anal. Biochem.* **2015**, *489*, 17-24. <https://doi.org/10.1016/j.ab.2015.08.002>.
- Muthamizh, S.; Suresh, R.; Giribabu, K.; Manigandan, R.; Kumar, S. P.; Munusamy, S.; Narayanan, V., MnWO<sub>4</sub> nanocapsules: Synthesis, characterization and its electrochemical sensing property. *J. Alloys Compd.* **2015**, *619*, 601-609. <https://doi.org/10.1016/j.jallcom.2014.09.049>.
- Durai, L.; Kong, C. Y.; Badhulika, S., One-step solvothermal synthesis of nanoflake-nanorod WS<sub>2</sub> hybrid for nonenzymatic detection of uric acid and quercetin in blood serum. *Mater. Sci. Eng. C-Mater.* **2020**, *107*, 110217. <https://doi.org/10.1016/j.msec.2019.110217>.
- Kathiravan, D.; Huang, B.R.; Saravanan, A.; Prasannan, A.; Hong, P.D., Highly enhanced hydrogen sensing properties of sericin-induced exfoliated MoS<sub>2</sub> nanosheets at room temperature. *Sens. Actuators B Chem.* **2019**, *279*, 138-147. <https://doi.org/10.1016/j.snb.2018.09.104>.